HIE-ISOLDE Project: The n-Converter/Fission Target Setup

Y. Kadi and A. Herrera-Martínez

The neutronic characteristics of the n-converter/fission-target system of the HIE-ISOLDE facility have been established (although not yet optimised) for a reference proton energy of 160 MeV. Several simulations have been carried out for different design requirements and different characteristics of the proton beam. An extensive comparison of the main physical parameters has also been carried out, in order to allow the optimal engineering design of the whole target station.

1. Introduction

The physics community that uses RIB (Radioactive Ion Beams), estimated to be about 1000 in Europe alone, requires diversity of ions species, diversity of beam energy, and high beam intensities. REX_ISOLDE already provides the first of these; the aim of HIE-ISOLDE is to achieve the second and the third. This requires developments in post-acceleration (the present energy restricts the application of REX to studies of light nuclei) and radioisotope selection as well as target-ion source development and charge-breeding to cope with the increase in proton intensity expected from LINAC4. It should be pointed out that HIE-ISOLDE would be transformed by the construction of a new proton driver such as the SPL and new target stations capable of accepting 100 μA proton beams [1] into a first-stage EURISOL that would allow achieving many of its physics goals. The project aims to improve the target and front-end part of ISOLDE to fully profit from potential upgrades of the existing CERN proton injectors e.g. faster cycling of the PS Booster and LINAC4.

In this note, we will present the results of recent simulations and analyses concerning the physics of the spallation target 160 MeV proton beam energy.

2. Physics of the Spallation Target

The converter/fission target system is the key component of most RIB facilities. Even in the HIE-ISOLDE facility, despite the relatively small power of the proton beam (a few kW), the development and design of the converter/fission target implies a detailed assessment of different aspects mutually interacting, from the physics of spallation – including neutron generation and distribution, reaction products yields and damage rates – to technological issues, such as choice of the most suitable material, power density distribution, heat removal, thermo-mechanics, fabricability, etc. In particular, accurate and rigorous assessment of

nuclear parameters under different physical conditions is the prerequisite for an optimal design of the target and its interaction with the front-end part.

This work aims at evaluating, using the Monte Carlo transport code FLUKA, the main neutronic and physical parameters such as yield and energy and angular distribution of the spallation neutrons, proton and neutron flux around the target, energy deposition, radiation damage, spallation product and fission product yields and radioactivity. The calculations have been performed for a 160 MeV proton beam impinging on a solid Tantalum n-converter. The performances and the impact on the target design of different shapes of the proton beam and geometrical configurations of the spallation target have also been assessed.

2.1 Geometrical description of the n-converter

Design studies previously carried out for the TRADE experiment [2] provided useful information for the preliminary design of the present n_converter. TRADE [3] was based on the coupling of a 140 MeV 1 mA accelerator with a subcritical TRIGA nuclear reactor core. The technical specifications of the coupling element, i.e. spallation target, were almost identical to those of the HIE-ISOLDE converter/target station.

The choice of tantalum as target material was driven by advantageous neutron yield and satisfactory mechanical properties even at high temperature. Tantalum has poorer thermal conductivity when compared with other common target materials, such as tungsten. Nevertheless this is not the only requisite for the choice, but also the following have to be accounted for: (i) low corrosion in water, specially in presence of water ionisation by protons; (ii) ductility even after irradiation; (iii) workability even to produce complicate shapes with good accuracy; (iv) good thermal contact and negligible differential thermal expansion in case of cladding; (v) easy fabricability of clad solutions.

However, the two experiments differ in the way the target is cooled. While TRADE target was conveniently cooled by convection with the water around the target, the heat deposited in the HIE-ISOLDE n_converter may only be removed by radiation and conduction (converter/target section is under vacuum). Consequently, the use of fins is suggested in order to enhance the cooling process (both radiating and conducting the heat to the externally cooled vessel), keeping the temperatures below its maximum value (~ 2000ºC).

The conical target geometry (Figure 1), combined with a Gaussian beam profile, was chosen to produce a homogeneous neutron (hence fission) and power density distributions.
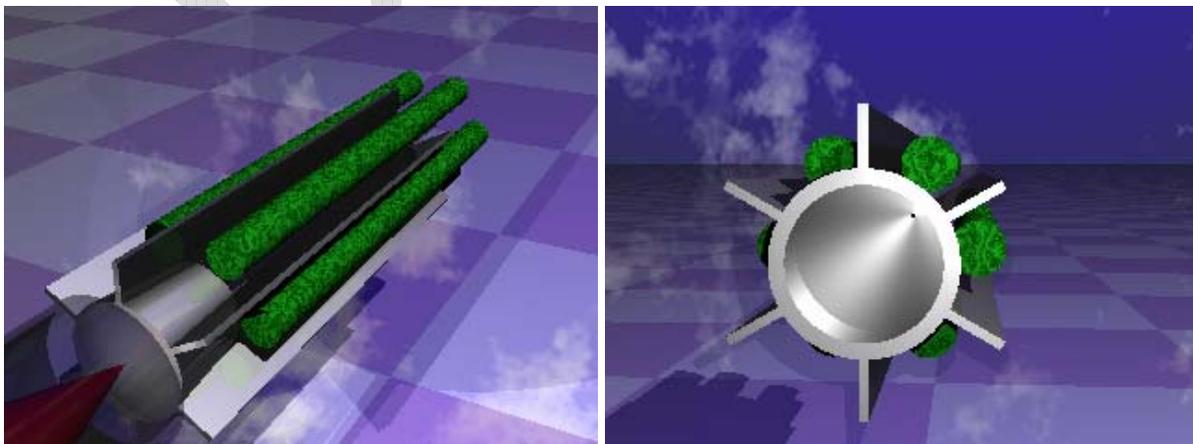
Fig.1 Schematic layout of the n-converter/target configuration

2.1.1 Inner geometry

The inner geometry (Figures 2a & 2b) is characterized by three conical cavities having different angles and total length equal to the active height of the surrounding fission target. The cone tip (lowest cone) is exposed to the highest power density for two reasons:

- the relevant proton current at the centre of the Gaussian distribution,
- the forward scattering of protons as a consequence of the conical angle steepness.

Fig.2a Mathematical optimization of the n-converter shape
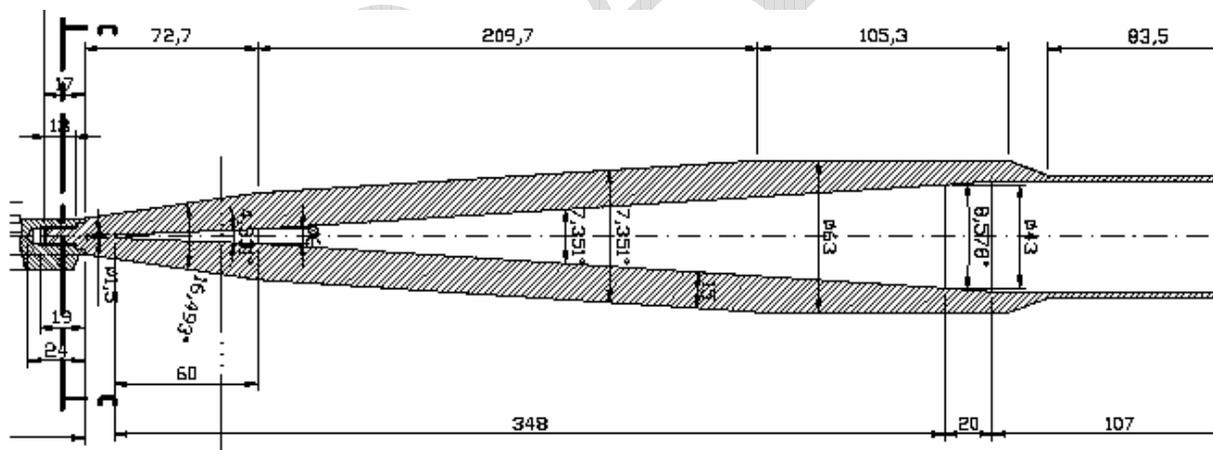
Fig.2b Inner shape of the n-converter body

Moreover, the deposited power at the tip of the cavity is very sensitive to the reduction of the sigma value of the gaussian beam, as shown in Figure 3 for 160 MeV proton energy. To better distribute the power, it is necessary to work out a small diameter at the tip of the cone. The former shape of the cone tip presented a series of drilled cylindrical bores which are now substituted by a smooth conical surface. This improvement was demonstrated to be feasible by the spark erosion technique up to a diameter of 1.5 mm as shown in Figure 4.
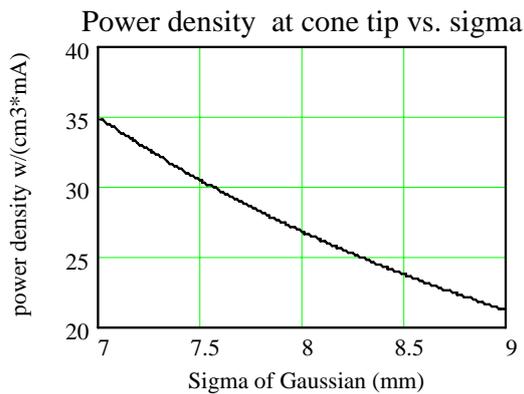
Fig.3 Power density at cone tip

Fig.4 Spark erosion bores in Ta

The conical wall angle of the lower cone, having predetermined the larger diameter as 6 mm, is identified by its length: the larger the length, the smaller is the linear power; nevertheless a maximum limit of 80 mm can be identified for fabrication reasons. The smooth conical surface strongly improves the power distribution of the lower cone which is more uniformly heated up. It is evident that, by increasing the cone length, one can decrease the power distribution at the tip, but this procedure implies an increase of linear power at the intermediate cone which should be balanced to better distribute the power in the whole spallation volume. Elastic thermo-mechanical calculations show that a best compromise can be reached with a lower cone length of 60 mm.

The intermediate truncated cone has an angle of 7.35° and receives the largest amount of power (77% of the total). In this region the forward scattering of protons mainly occurs, therefore, in order to widen its angle, a conical region having steeper angles was located below its position.

The upper truncated cone is very short (21 mm) and has the function to directly connect the target to the beam transport line; the tails of the Gaussian profile are here truncated. This cone has the largest angle to keep constant the axial position of the beginning of the spallation process, even in presence of small radial errors. The impinging power is relatively low as shown by the calculated axial distribution of power.

2.1.2 Outer geometry

The typical range of 160 MeV protons, being stopped in Tantalum is ~ 21 mm and a thickness of 5 mm was assumed in the design as a compromise to assure the radial heat removal without intolerable thermal stresses. At the lowest cone the 15 mm thickness produces excessive thermal stress and has to be reduced. This is due to the shape factor "$1/\ln(re/ri)$" which affects the integration of Fourier Law in axial-symmetric geometries. In Figure 5 the comparison between the shape factors, is reported for the lowest cone in case of constant thickness and reduced thickness.
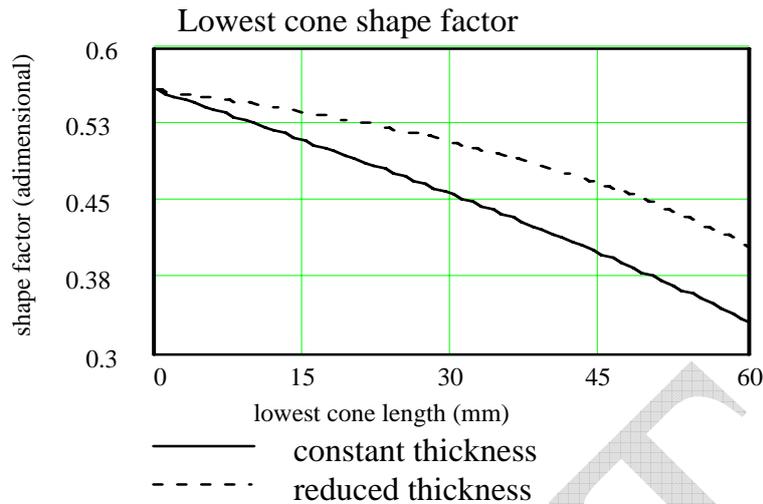
Fig.5 Variation of the shape factor versus lowest con length

2.2 Nuclear performance of the target

The main neutron physic parameters of the n-converter such as neutron yield and energy spectra, power deposition, material damages and spallation and fission product distributions are evaluated by the probabilistic transport code FLUKA [4].

The impact of different target parameters (material choice, geometry of the proton beam) has been studied. While the neutron yield and spectra are mainly related to the nuclear behavior of the system, energy deposition is directly related to the thermo-mechanics of the target and its cooling capabilities, which determine its lifetime.

2.2.1 Neutron production

The main goal of the spallation target is the neutron production. Calculations performed for 160 MeV protons distributed according to a Gaussian profile (as discussed in section 2.1.1) on thick (conical versus cylindrical) and thin (conical) geometries of the Tantalum n-converter show that the neutron yield (Table 2) is not affected significantly by the target geometry since the protons are almost at the end of their range when they leave the converter. Even in the "thin" geometry, the material thickness (3 mm in the radial direction) is sufficient to allow the whole spallation reactions to take place inside the converter part.

Table 2 Neutron production process

Target type	Neutron yield
Thick target 10 cm long (cylindrical)	0.99 n/p
Thin target 3 mm (conical)	0.95 n/p
Thick target 10 mm (conical)	1.02 n/p

The neutron flux distribution for the thick target configuration is reported in Figure 6. The region of maximum production lies in the median plane of the fission target. In order to achieve a better efficiency in the use of the source neutrons (flatter distribution of the neutrons along the length of the fission target), it is necessary to incline the target body by a few degrees to reduce the gap with the n-converter.
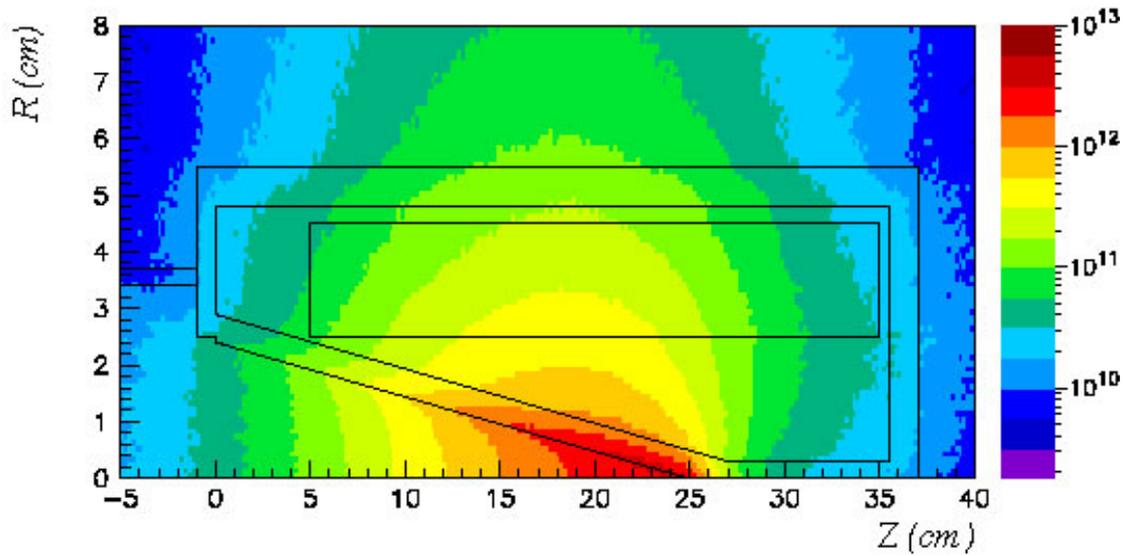
Fig.6 Neutron flux distribution in (n/cm^2/s) per kW of beam

The neutron spectra shown in Figure 7 are the result of a complete simulation performed with the target described above (no contribution from reflected neutrons). In reality the contribution by the reflected neutrons is not negligible and will result in additional activation of the n-converter/fission target setup. For high energies, it is possible to distinguish the well-known peak at 1 MeV related to evaporation phase of the spallation process. A second broader peak is clearly distinguishable at higher energies (above a few tens of MeV), which is related to the INC (Intra-Nuclear Cascade) phase of the spallation process.
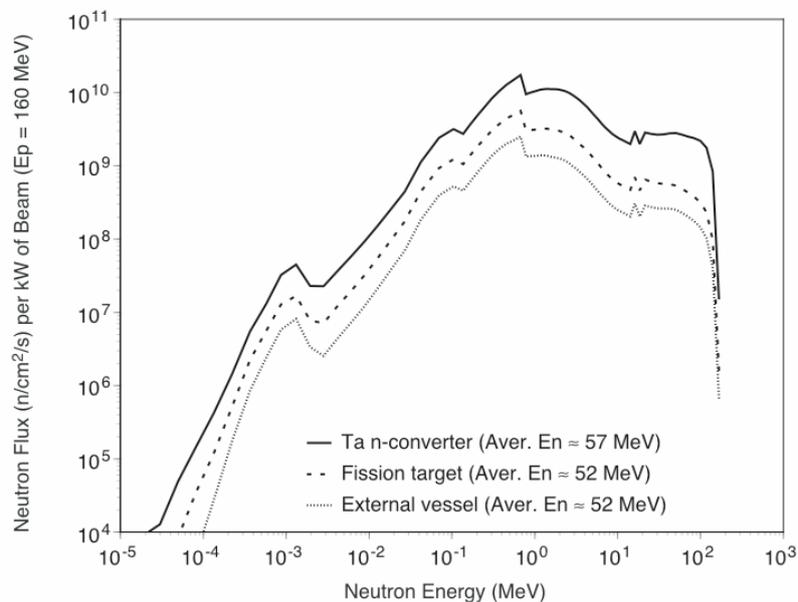
Fig.7 Neutron flux spectra at several locations inside the converter/target station in (n/cm^2/s) per kW of beam. The average energy of the high-energy neutrons (>20MeV) is also reported

Overall, the integrated flux of neutrons escaping the target (i.e. entering the front-end section) is reduced by a factor 10 as a result of the successive attenuation in the solid Ta converter body but also in the thick fission targets surrounding it.

Nevertheless, the high-energy tail of the neutron distribution when entering the front-end structures is still present and the high-energy neutrons (> 10 MeV), only slightly moderated, still represent ~ 9% of the spallation neutron population with an average energy of about 50 MeV, as shown in Table 3.

Table 3 Relative neutron energy distribution

Energy groups	Neutrons escaping from vessel (% of flux)	Neutrons inside fission target (% of flux)
0 – 1 eV	–	–
1 eV – 1 keV	0.1	0.1
1 keV – 1 MeV	46.1	45.0
1 MeV – 10 MeV	45.2	46.6
> 10 MeV	8.9	8.3

These high-energy neutrons are very hard to shield, and contribute to a certain extent to the radiation damage of the inner structure of the target station and also to the ambient dose in the target building should they leak out. Moreover, they may react with the target station cooling circuit and produce N^{16} through (n,p) reactions on O^{16} which has a threshold of ~ 10 MeV and whose cross section peaks at 0.15 barn compared to the 0.2 barn total cross section of H.

This is further illustrated in Figure 8, which shows the spatial distribution of the high-energy component (> 20 MeV) of the neutron flux in the converter/target section.
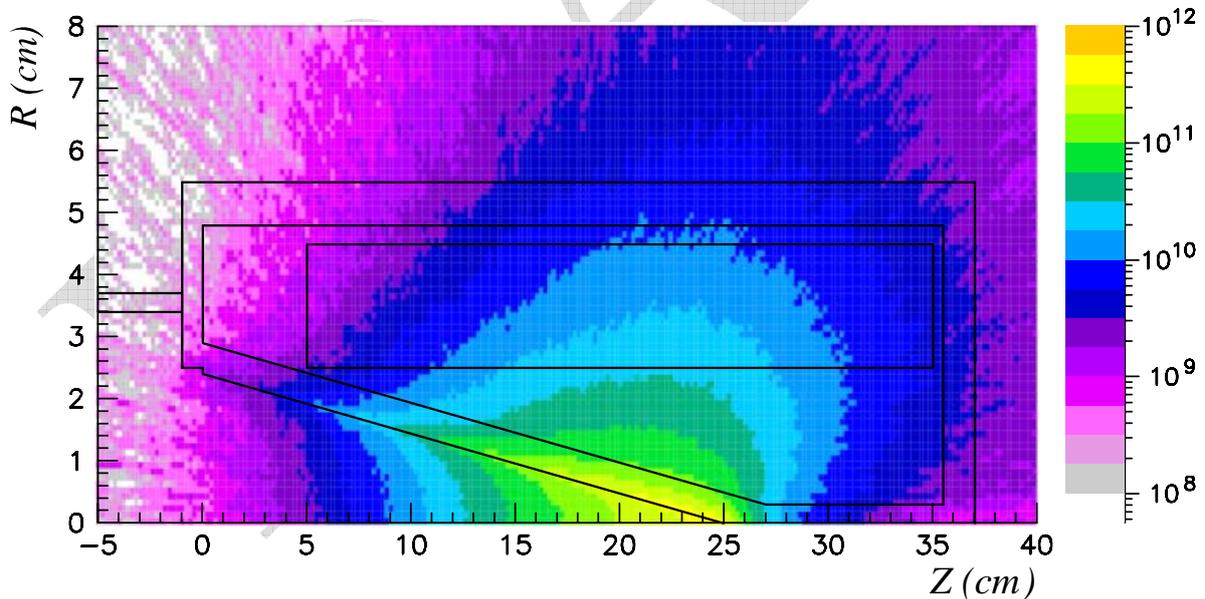
Fig.8 Neutron flux distribution of the > 20 MeV in (n/cm^2/s) per kW of beam

We estimate the flux of neutrons > 20 MeV reaching the front-end section to be of the order of 10^{10} n/cm^2/s per kW of beam and up to 10^9 in the bottom part of the target vessel. These neutrons tend to be forward peaked (> 50°), contrary to the low-energy neutrons which are more or less centred along the target mid-plane (Figure 6). On the other hand, any beam offset will produce an axial shift of the high-energy neutron distribution that can be easily

monitored by placing at several locations along the height of the target a series of detectors sensitive to the recoils generated by the high-energy component of the neutron flux (> 1 MeV).

These high-energy neutrons can penetrate deep inside the front-end section and surrounding biological shield contributing therefore to the ambient dose therein.

2.2.2 High-energy proton leakage

The release of protons out of the spallation target causes the production of unwanted radionuclides in the front-end section of the facility and contribute also to local heating in the fission target, therefore it has to be taken into account to identify the n-converter acceptability and if possible minimized.

The primary proton flux distribution for the thick target configuration is illustrated in Figure 9. The fraction of protons escaping the n-converter/target section is almost negligible apart from the upper part of the converter section (direct connection to the beam transport line) where the tails of the Gaussian profile are truncated. In any case the majority of the protons escaping the spallation target are either stopped by the fins, which guaranty the thermal contact with the external vessel, or by the fission targets surrounding the solid n-converter. Very few manage to escape through the external vessel and reach the front-end structures or are backscattered into the vacuum beam pipe.
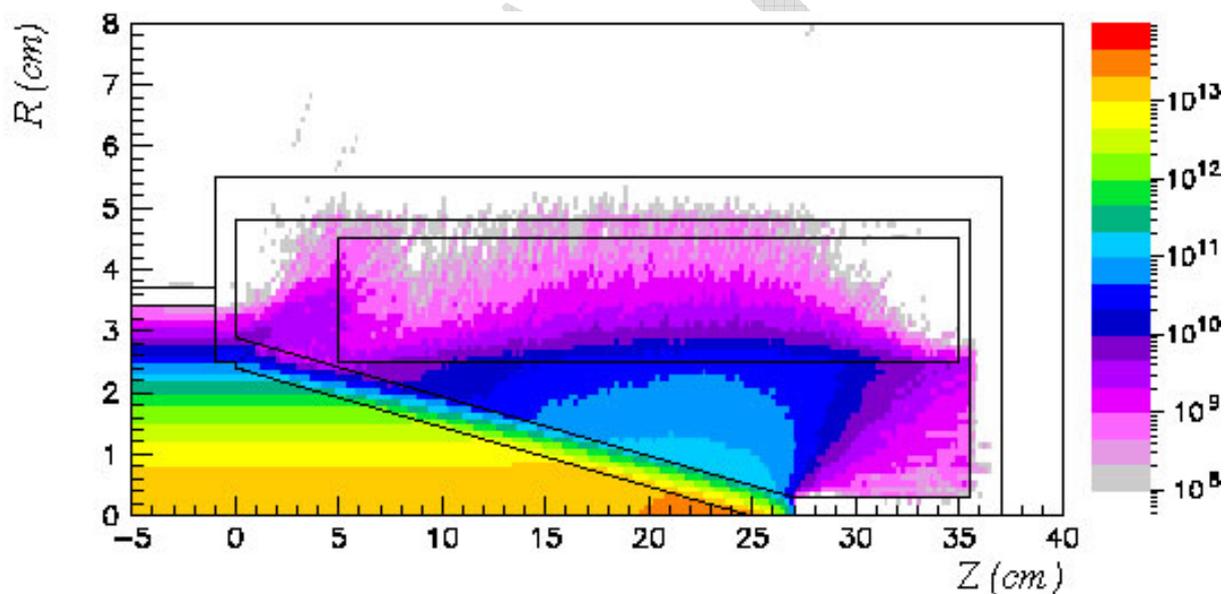
Fig.9 Primary proton flux distribution in (p/cm^2/s) per kW of beam

Figure 11 shows the spectra of protons (both primary and secondary) escaping from the target and from the target vessel. The proton flux above 10 MeV escaping from the target vessel, has been reduced by almost three orders of magnitude. The high-energy tail, which is still present, but at a much reduced scale, corresponds to those protons cut out from the tail of the Gaussian profile at inlet. The low-energy proton flux results mostly from high-energy neutron (n,Xp) reactions in carbon and in tantalum.
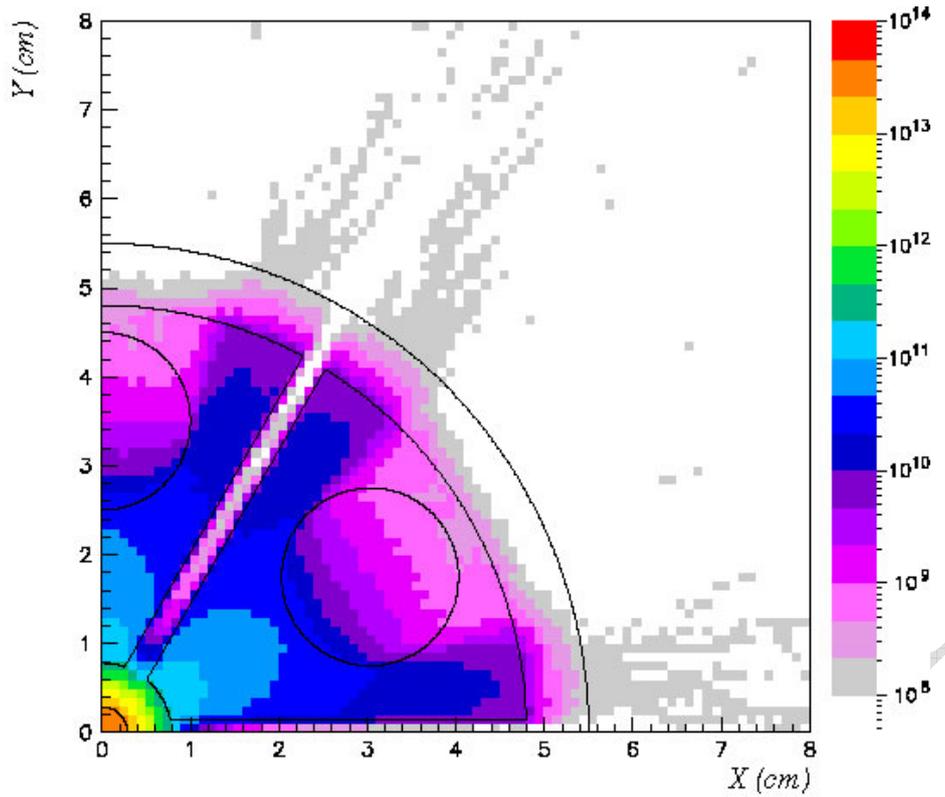
Fig.10 Primary and secondary proton flux distribution in (p/cm^2/s) per kW of beam
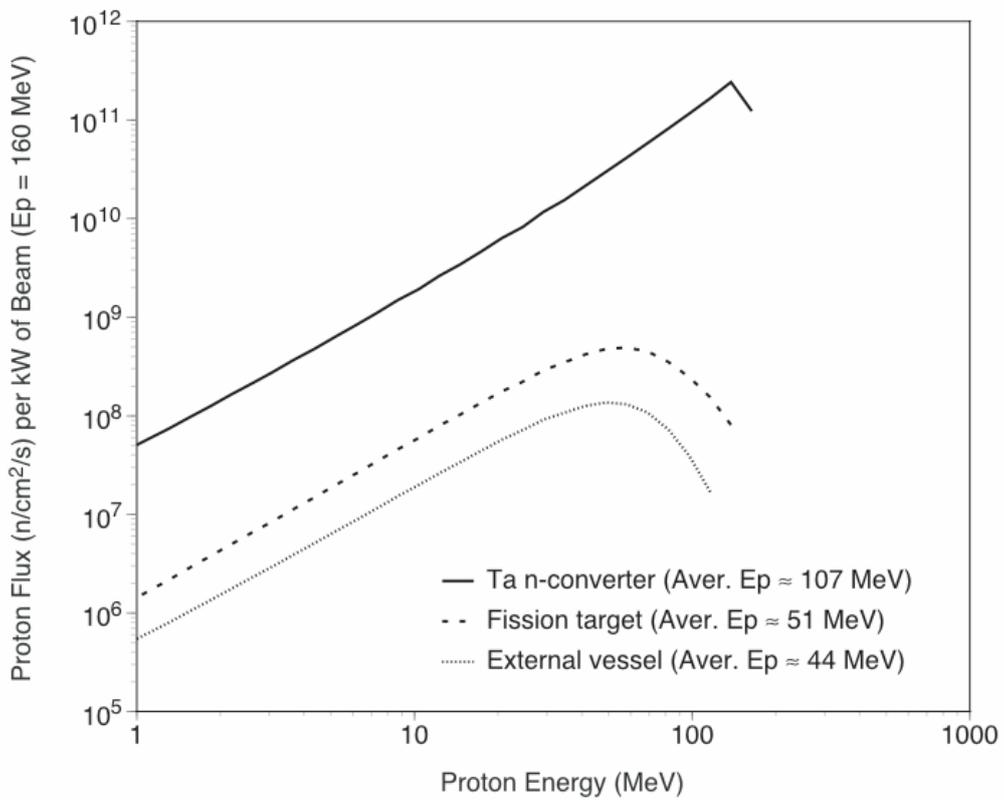
Fig.11 Proton flux spectra at several locations inside the converter/target section in (p/cm^2/s) per kW of beam

2.2.3 Fission product yields and activation of the solid Ta n-converter

In the solid Ta n-converter as well as in the fission targets surrounding, spallation, fission and activation products (no contribution from the reflected neutrons) are continuously produced; their amount was calculated and reported in Figures 12a and 12b.
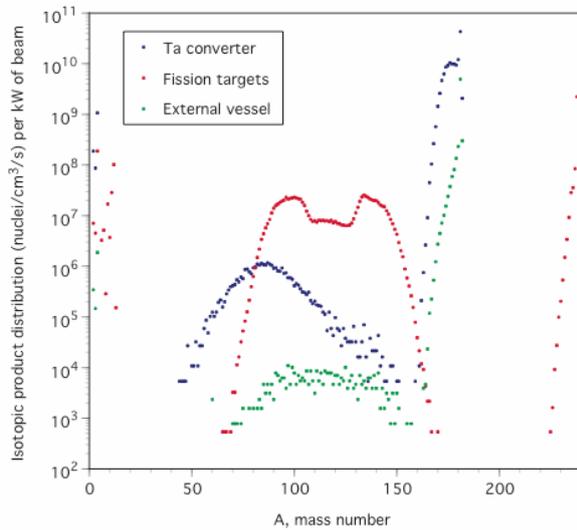
Fig.12a Yield of residual products in UCx vs. A in (nuclei/cm^3/s) per kW of beam
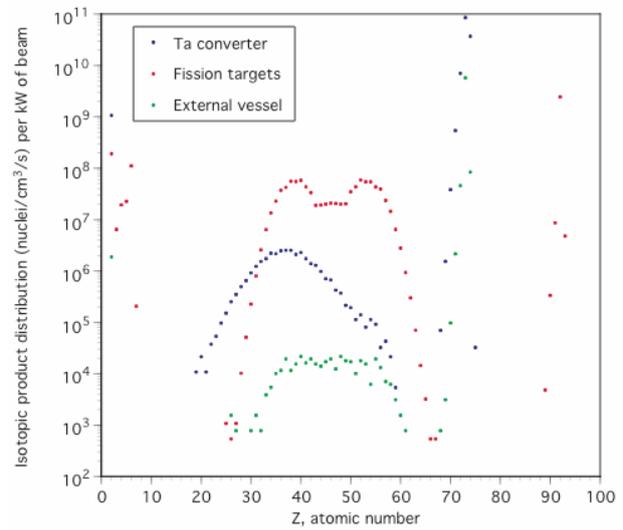
Fig.12b Yield of residual products in UCx vs. Z in (nuclei/cm^3/s) per kW of beam

The spatial distribution of the fissions occurring in the UCx cylindrical targets is shown in Figure 13. These fissions, whose density peaks at ~ 3x10^9 cm^{-3}s^{-1} per kW of beam, are not homogeneously distributed inside the UCx rods, indeed most of them take place along the side of the rod which is facing the Ta n-converter. Further optimization of the fission target geometry is therefore required in order make this distribution more uniform.
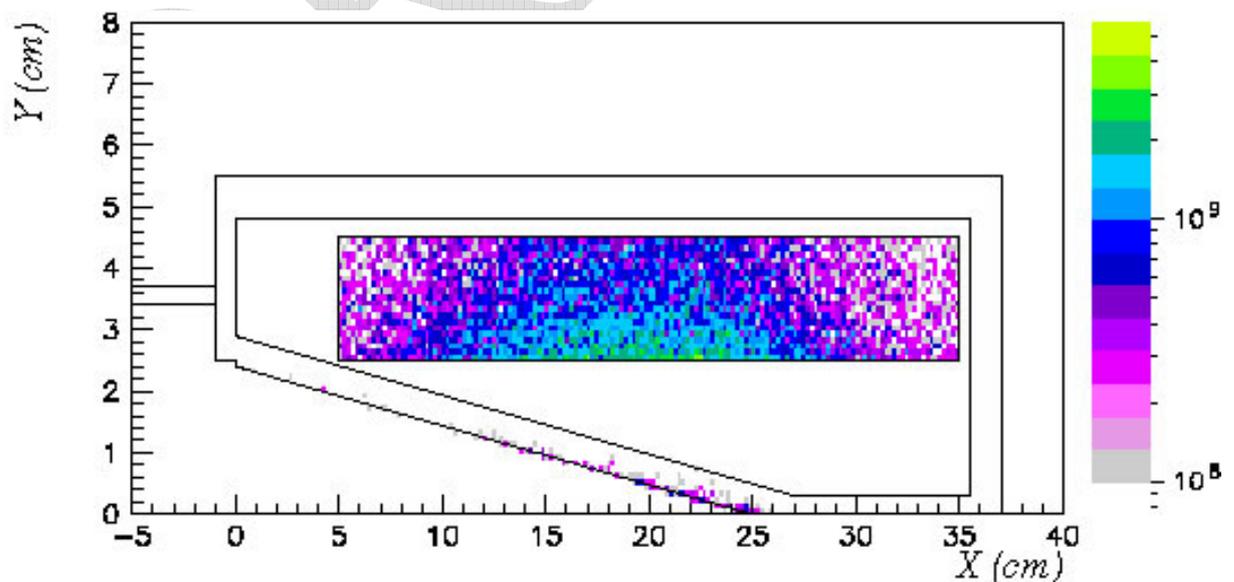
Fig.13 Fission density distribution in the converter/target station in (fission/cm^3/s) per kW of beam

The fission targets are formed by a 5 g/cm^3 compound of three atoms of carbon per atom of uranium (natural U). The volume of each one of the six cylindrical fuel pins is 94.25 cm^3, with a radius of 1 cm. Table 4 shows the average yields in the fuel pins for some isotopes of interest.

Table 4 Isotopic yields in the UC$_x$ fuel rods (Ions/cm^3/µC).

28-Ni (A)	Ions/cm^3/µC	Error (%)	31-Ga (A)	Ions/cm^3/µC	Error (%)
70	4.31E+02	48.7	72	1.72E+02	67.4
71	1.72E+02	67.4	73	2.58E+02	53.9
72	1.72E+02	67.4	74	6.87E+02	42.2
73	4.31E+02	39.8	75	2.67E+03	16.2
74	3.45E+02	45.6	76	3.88E+03	14.5
76	8.61E+01	97.3	77	1.09E+04	7.3
50-Sn (A)	**Ions/cm^3/µC**	**Error (%)**	78	1.40E+04	8.9
113	8.61E+01	97.3	79	2.93E+04	5.8
117	1.72E+03	23	80	2.38E+04	5.9
119	1.79E+04	9	81	2.45E+04	7
121	8.80E+04	4.1	82	9.80E+03	8.4
123	2.36E+05	2.4	83	5.17E+03	14.2
125	3.25E+05	1.7	84	2.15E+03	17.4
126	4.19E+05	1.6	85	5.17E+02	42.5
127	3.24E+05	1.5	86	1.72E+02	67.4
128	4.38E+05	1.5	**36-Kr (A)**	**Ions/cm^3/µC**	**Error (%)**
129	5.04E+05	1	85	7.30E+03	12.1
130	7.68E+05	1.1	87	9.49E+04	2.2
131	8.49E+05	1	88	3.84E+05	1.4
132	6.24E+05	1.5	89	6.02E+05	1.1
133	2.23E+05	1.7	90	1.18E+06	0.7
134	5.20E+04	4.8	91	1.34E+06	0.8
135	7.05E+03	12.1	92	1.20E+06	0.7
136	4.31E+02	48.7	93	6.30E+05	1.1
			94	3.59E+05	1.7
			95	7.86E+04	2.8
			96	3.17E+04	6.7
			97	4.22E+03	15
			98	3.01E+03	16.4
			100	1.72E+02	67.4

Burn-up calculations have been carried out to estimate the activation of the Tantalum spallation target. As shown in Figure 14, it is worth noting that the activity of the spallation target (expressed in Ci per year of irradiation, i.e. 2000 hours, per kW of beam) is dominated by the decay of the spallation products, mostly Hf, Lu and Yb isotopes. At longer times (> 40 years) tritium is the only isotope of importance. Note that tritium is the only troublesome volatile produced in the spallation target.
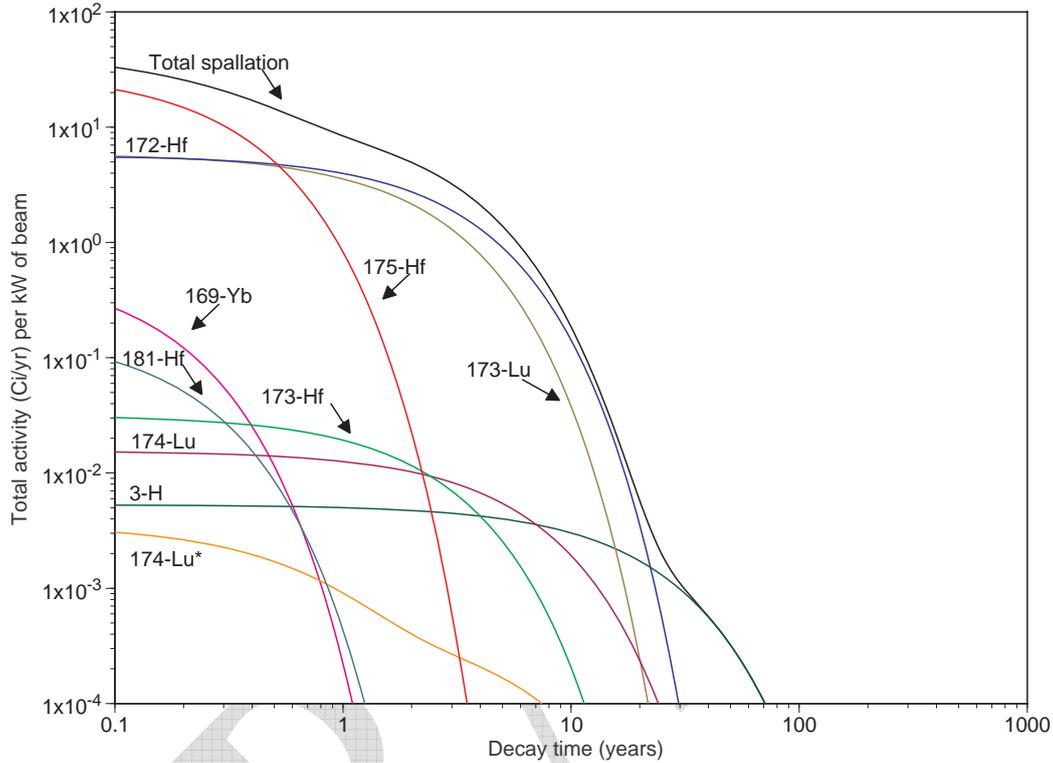
Fig.14 Evolution of the radioactivity of the Tantalum spallation target as a function of time in (Ci/yr) per kW of beam

2.2.4 Radiation damage

The particle flux spectra generated by FLUKA [4] can be used to estimate the heating and damage to structural materials by protons and neutrons with energy above and below 20 MeV. Indeed, one can consider separately the high-energy portion of the spectrum, due to the primary proton shower, with its intensity proportional to the beam current, and a lower energy region associated with the fission targets.

In practice, we have evaluated:

$$\frac{\delta(dpa)}{\delta t} = \frac{\langle \sigma E_a \rangle}{\frac{2 E_d}{\eta}} \cdot \phi \cdot 10^{-21} \text{ [dpa/s]} \qquad \text{Eq.(1)}$$

where $\langle \sigma E_a \rangle$ is the damage energy production cross section (barn-keV), E_d is the energy required to displace an atom from its lattice position (eV), $\eta = 0.8$ is the collision efficiency factor and ϕ is the particle flux (cm^{-2}.s^{-1}).

As regards the damage induced by high-energy particles (> 20 MeV), we have used data that provides values for proton- and neutron-induced displacement cross sections as calculated using the default physics models in MCNPX [5] and illustrated in Figure 15.
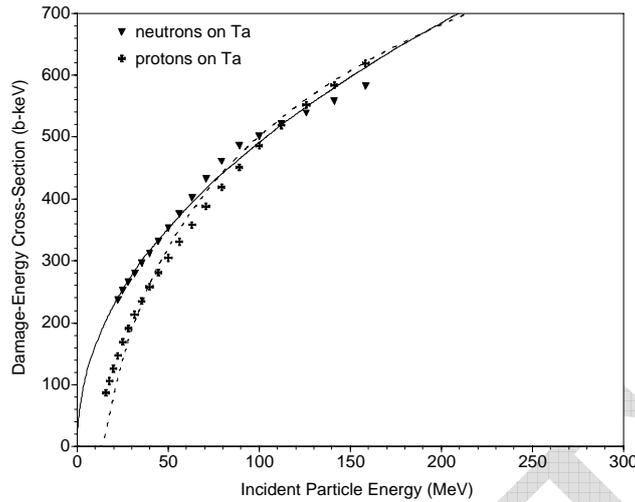
Fig.15 Neutron and proton-induced damage-energy cross sections for Tantalum in (barn-keV)

Table 5 indicates the values of the integrated flux in the spallation target unit, due to high-energy particles (HE).

Table 5 Integrated flux per kW of beam power in different parts of the target station

Region	HE proton Flux (part/cm^2.s)		HE neutron Flux (part/cm^2.s)	
	Max	Ave	Max	Ave
Ta n-converter	$3.0x10^{13}$	$1.2x10^{12}$	$5.5x10^{11}$	$5.1x10^{10}$
UC$_x$ target	$3.1x10^{10}$	$1.6x10^9$	$3.4x10^{10}$	$1.7x10^{10}$
Ta fins	$\sim10^9$	$\sim10^8$	$1.6x10^{11}$	$3.1x10^{10}$
Ta external vessel	$\sim10^7$	$\sim10^7$	$\sim10^{10}$	$\sim10^{10}$

The gas production and the displacement rates (dpa/yr) obtained using Eq. (1) together with the particle fluxes listed in Table 5 are reported in Table 6 for the same operating conditions as those listed above, that is per kW of beam and for an expected duty factor of the HIE-ISOLDE facility of about 22% (2000 hours).

Table 6 Gas production and the displacement rates per kW of beam

Target (Ta)	Average Prot. Ener (MeV)	Average Neut. Ener (MeV)	H$_3$ Production (appm/dpa)	He Production (appm/dpa)	HE proton (dpa/yr)		HE neutron (dpa/yr)	
					Max	Ave	Max	Ave
Ta n-converter	107	57	0.01	0.12	1.1	0.04	0.016	0.002
UC$_x$ target	51	52	-	0.12	-	-	0.001	-
Ta fins	50	51	-	-	-	-	0.004	0.001
Ta ext. vessel	44	52	-	-	-	-	-	-

The particle damage are entirely dominated by the high-energy protons and localized on the inner skin of the spallation target with a maximum situated at the tip of the inner cone. It is further reduced when the sigma of the proton beam distribution increases.

2.2.5 Energy deposition

While the previous parameters were mainly related to the nuclear behaviour of the system, energy deposition is directly related to both the thermo-mechanics of the target and its cooling capabilities, which determine its lifetime. The power density distribution, is a central factor in the thermal design of spallation targets.

The largest value of the power density, which is equal to 250 W/cm^3 per kW of beam of 160 MeV protons, is found at the tip of the conical cavity at the bottom of the target, as shown in Figure 16. Very little heat is deposited in the fission target or in the thermal contacts (< 1 W/cm^3 per kW of beam) by the primary proton beam, as illustrated by Figure 17.
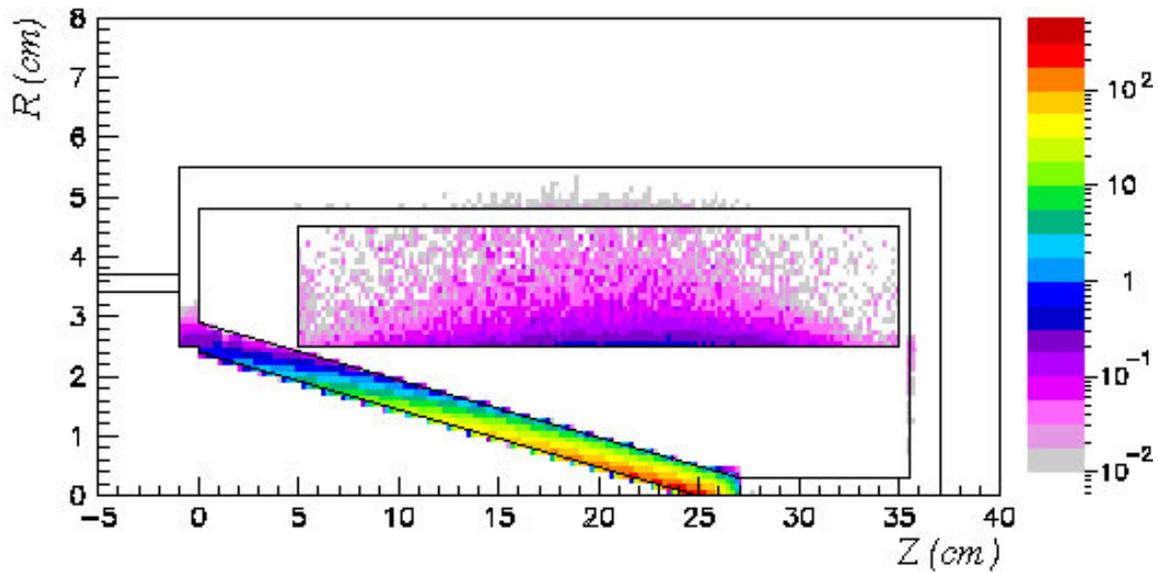
Fig.16 Power deposition in the tip region in (W/cm^3) per kW of beam at 160 MeV
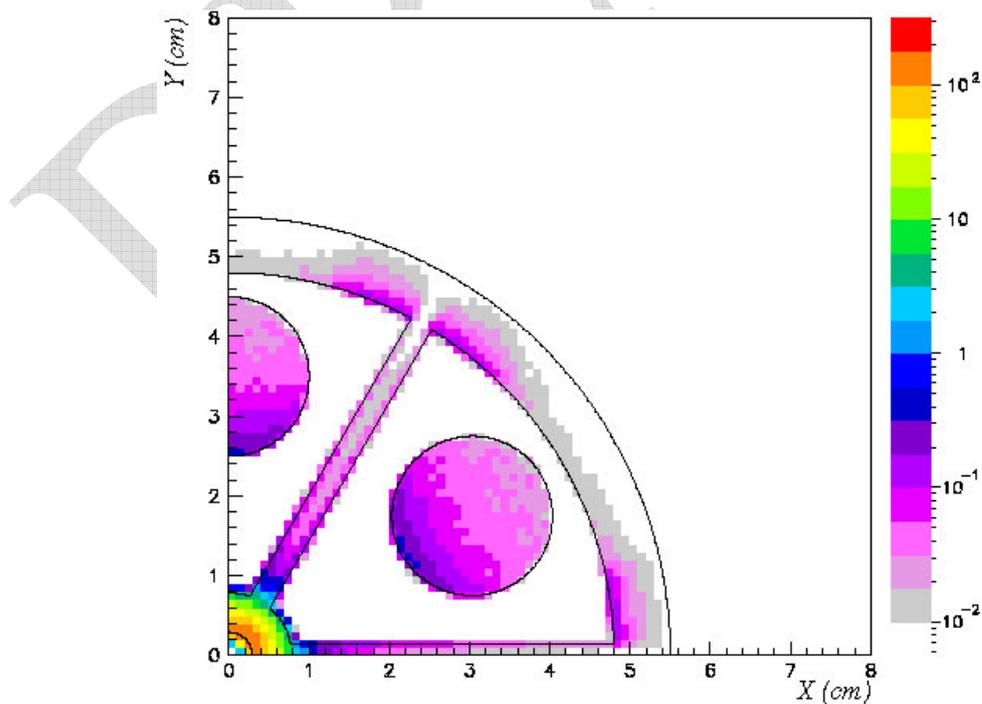
Fig.17 Power deposition in the entire target section in (W/cm^3) per kW of beam at 160 MeV at 22 cm from the top of the cone.

The distribution inside the target reveals a rather homogenous behaviour with an average power density of ~ 4 W/cm^3 per kW of beam. A discontinuity is observed in the aluminium beam pipe (where the tail of the Gaussian profile is cut out) and in the upper truncated cone region of the target where the cone has the largest angle to keep constant the axial position of the spallation neutron source distribution, even in presence of small beam offsets. However, the impinging power there is relatively low.

References

[1]   M. LINDROOS, private communication, CERN (2005).

[2]   C. KRAKOWIAC et al., "The TRADE Solid Target System Design", in Proc. of the Int. Conf. On Advanced Nuclear Energy and Fuel Cycle Systems, GLOBAL 2003, New Orleans, Louisiana, USA, November 16-20, 2003.

[3]   The Working Group on TRADE: The TRIGA Accelerator Driven Experiment, Final Feasibility Report, ENEA, March 2002.

[4]   A. FASSO' et al., "FLUKA: Status and Prospective for Hadronic Applications", Proceedings of the MonteCarlo 2000 Conference, Lisbon, October 23-26 2000, A.Kling, F.Barao, M.Nakagawa, L.Tavora, P.Vaz - eds. , Springer-Verlag Berlin, p.955-960 (2001).

[5]   E. PITCHER, private communication, LANL (2003).